Journal of Zhejiang University-SCIENCE A (Applied Physics & Engineering)
ISSN 1673-565X (Print); ISSN 1862-1775 (Online)
www.zju.edu.cn/jzus; www.springerlink.com
E-mail: jzus@zju.edu.cn

Determination of particle size distribution by multi-scale analysis of acoustic emission signals in gas-solid fluidized bed*

Cong-jing REN†, Jing-dai WANG, Di SONG, Bin-bo JIANG, Zu-wei LIAO†‡, Yong-rong YANG

(*State Key Laboratory of Chemical Engineering, Department of Chemical and Biochemical Engineering, Zhejiang University, Hangzhou 310027, China*)

†E-mail: seasonrcj@zju.edu.cn; liaozw@zju.edu.cn

Received Sept. 9, 2010; Revision accepted Dec. 16, 2010; Crosschecked Jan. 28, 2011

Abstract: Particle size distribution (PSD) is an important parameter in the process of fluidization, and it always plays a crucial role in a gas-solid fluidized system. A PSD model for on-line PSD determination based on acoustic emission (AE) measurement was developed according to the mechanism of particle collision with the inner wall of the cylinder and multi-scale wavelet decomposition analysis. This PSD model illuminates the quantitative relationship between the energy percentage of AE signals for different scales and the PSD, which indicates the feasibility of the application of the PSD model. Experiments were undertaken both in lab and plant gas-solid fluidized setup with polyethylene particles, and the parameters of the PSD model were calibrated and revised. The experimental conditions and results proved that the PSD model was suitable for on-line measurement and was sufficiently sensible and accurate. Concerning agglomeration, the PSD model also showed exact serviceability on detecting the onset of agglomeration by abnormal PSD, and the result agreed with that from the radiation method. Ultimately, AE measurement was found to be a reliable and credible means for understanding the PSD information that affects the behavior of a system, which can provide valuable guidance for practical applications.

Key words: Particle size distribution (PSD), Acoustic emission (AE), Fluidized bed, Multi-scale, Agglomeration
doi:10.1631/jzus.A1000396 **Document code:** A **CLC number:** TQ021.1

1 Introduction

Particle size distribution (PSD) is a fundamental parameter in the process of fluidization, and it has become increasingly attractive in many different industrial applications during the past decade. There are many situations where the knowledge of PSD during fluidized bed operation is desirable. For example, in the mining and mineral processing industry, on-line measurements of coarse PSDs have been used to monitor the size distributions of crushing/grinding products (Lange, 1988; Lin *et al*., 1995; 2000), and in the rock blasting industry, blast control modeling requires information on the blasted PSDs (Hunter *et al*., 1990; Monoro and Gonzalez, 1993; Franklin and Katsabanis, 1996).

In most cases, PSD has a strong influence on the hydrodynamics and related characteristics of gas-solid fluidized beds, such as mixing and conversion. Most powder handling/processing operations rely on the measurement of size distributions, which is a key factor in improving process efficiency (Fuerstenau and Kenneth, 2003). Therefore, it is an essential quality control characteristic of many industrial product specifications that often affecting important bulk characteristics; e.g., the PSD is a major determinant regarding flow properties.

As a means of obtaining the correct method of monitoring PSD, many applications have been presented. However, conventional PSD monitoring technologies, such as sieving, image analysis of prepared samples, laser diffraction, and laser backscattering, do not provide the monitoring capability

‡ Corresponding author

* Project supported by the National Natural Science Foundation of China (Nos. 21076180 and 20736011), and the National High-Tech R&D Program (863) of China (No. 2007AA04Z182)

necessary to achieve on-line PSD control especially for systems in which the particles are highly non-spherical (Braatz, 2002). The sieving method can be tedious and time-consuming particularly when handling large amounts of fine particles (Allen, 1990; Fuerstenau and Kenneth, 2003). The laser diffraction overestimates the broadness of the spherical diameter distribution for high-aspect-ratio particles due to orientation effects and the spherical models used to interpret the diffraction data (Naito *et al.*, 1998; Xu and Guida, 2003). The chord length distribution measured using laser backscattering can be inverted theoretically to obtain the PSD for high-aspect-ratio particles, but the inversion is highly ill-posed (Worlitschek *et al.*, 2005; Larsen *et al.*, 2006) and requires assumptions regarding the particle shape. To summarize, the shortcomings of the methods used at present limit their applications in practice. Therefore, it is of crucial importance to find an effective on-line measurement to monitor PSD in gas-solid fluidized beds.

Often, an on-line technique should both be fast and robust in delivering the results, typically for a large number of measurements, and reliable in having high levels of accuracy and precision. In comparison with those methods mentioned above, passive acoustic emission (AE) signals, which are generated as a result of the collision by particles and sampled by accelerometers, have much information about the size and movement of fluidized particles (Cody *et al.*, 1996; 2000; Halstensen and Esbensen, 2000; Boyd and Varley, 2001; Mylvaganam, 2003; Jiang *et al.*, 2007; Ren *et al.*, 2008). In other words, AE signals are sensitive and selective to particle movement, which makes it possible to monitor information of particles by analyzing AE signals. Also, AE measurement is proved to be a reliable and well-established technique for machinery condition, and has been proved sensitive, environmentally friendly, non-invasive, and suitable for on-line measurements (Wang *et al*., 2007; 2010; He *et al*., 2009). In this paper, the AE method and multi-scale wavelet analysis were applied, and a PSD model was obtained. To our delight, the results demonstrated that AE technique and energy analysis can serve as reliable tools to monitor PSD both in cold-model equipment and pilot-scale setup.

2 Particle size distribution model based on acoustic emission method

For homogeneous particles with the same diameter D and mass m impact on an area ΔA of the internal wall of a fluidized bed, the resultant force $F(t)$ is given by

$$F(t)=\sum_{i=1}^{n}2mv_i\delta(t-t_i), \tag{1}$$

where the Dirac delta function $\delta(t)$ related with time t, t_i is the arrival time of the ith particle, and v_i is the vertical velocity of the ith particle colliding with the wall. Thus, there are $f_p{\cdot}T$ impacts in the time interval T, where f_p is the mean arrival rate of the particles on the area ΔA. The mean force of particles in the unit time can be written as

$$<F(t)>=\frac{1}{T}\int_0^T F(t)\mathrm{d}t=\frac{2mv}{T}\int_0^T\sum_{i=1}^{n}\delta(t-t_i)\mathrm{d}t, \tag{2}$$

where v is the mean vertical velocity of all particles colliding with the wall, and n is the particle number. For $\int_0^t\sum_{i=1}^{n}\delta(t-t_i)\mathrm{d}t=f_pt$, $<F(t)>$ can be described as

$$<F(t)>=2mvf_p. \tag{3}$$

This relationship should be familiar as the starting point for the calculation of the pressure exerted on the wall of a vessel by the impact of the molecules in a gas. The acoustic pressure P_{AE} can be written by

$$P_{AE}=\eta\frac{<F(t)>}{\Delta A}, \tag{4}$$

where η denotes the efficiency of the impacted pressure that transforms to the acoustic pressure. Assume that the concentration of the particles impacted on the wall is C, which is in inverse ratio to the projection area of the particles to the wall; that is, $C=\xi/D^2$, where ξ is the coefficient. The mean arrival rate of the particles on the area ΔA, f_p, is given by

$$f_{\mathrm{p}} = C\frac{\Delta A v}{\Delta A} = Cv. \tag{5}$$

Therefore, the average acoustic energy flux in the unit time can be written as

$$J = P_{\mathrm{AE}}\Delta A v = 2\eta m v^2 f_{\mathrm{p}} = 2\xi\eta m v^3 / D^2. \tag{6}$$

The acoustic energy E is given by

$$E = \int_0^T J\mathrm{d}t = \int_0^T \frac{\pi}{3}\xi\eta\rho_{\mathrm{s}} v^3 D\mathrm{d}t, \tag{7}$$

where the acoustic energy E is the function of particle diameter D, density ρ_{s}, and time interval T. That is to say, if ρ_s and T are invariable, the acoustic energy E is associated with particle diameter D, even the PSD.

For j component particles that the jth component particle mean size is D_j with the mass fraction x_j impact onto the inner wall, the acoustic energy for the mixture E_{mix} can be written as (Haar, 1954)

$$E_{\mathrm{mix}} = \sum_{j=1}^{J} E(D_j)x_j \quad \text{or} \quad \sum_{j=1}^{J}\frac{E(D_j)}{E_{\mathrm{mix}}}x_j = 1, \tag{8}$$

where $E(D_j)$ is the acoustic energy of the particle j. For j component particles, j kinds of formulas are needed at least to obtain PSD. In this study, Daubechies 2 wavelet is chosen to analyze the experimental data. By wavelet decomposition with the Mallat algorithm as shown in Fig. 1, the original signals will be decomposed into k scales of orthogonal approximation and detail functions, and the number k (k=1, 2, …, K) reflects the decomposition level.

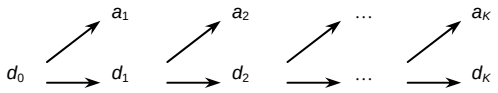

Fig. 1 Signal decomposition using the wavelet Mallat algorithm

a_k: approximation signal; d_k: detail signal (k=1, 2, …, K)

Define the energy of AE signals in all scales decomposed by wavelet transform as follows:

$$E_k^{\mathrm{a}}(D_j) = \sum_{t=1}^{T} a_k^2,\ E_k^{\mathrm{d}}(D_j) = \sum_{t=1}^{T} d_k^2, \tag{9}$$

where $E_k^{\mathrm{a}}(D_j)$ and $E_k^{\mathrm{d}}(D_j)$ represent the energies of approximation signal components and detail signal components in the kth scale of the jth component particle, respectively, and t is the time of the signal from 1 to T. Then, the energy of the jth component particles would be given by (Peng, 2000)

$$E(D_j) = E_k^{\mathrm{a}}(D_j) + \sum_{k=1}^{K} E_k^{\mathrm{d}}(D_j). \tag{10}$$

For the independency characteristic of acoustic waves (Wu, 1999), their properties (frequency, amplitude, etc.) remain invariable when several waves are mixed. Consequently, we could assume the conservation of the energy in each scale, and the relationship between the energy of particle j and the mixture can be written as

$$\begin{cases} \sum_{j=1}^{J}\lambda_j\frac{E_k^{\mathrm{a}}(D_j)}{E(D_j)}x_j = \frac{E_{\mathrm{mix},k}^{\mathrm{a}}}{E_{\mathrm{mix}}},\ k = K, \\ \sum_{j=1}^{J}\lambda_j\frac{E_k^{\mathrm{d}}(D_j)}{E(D_j)}x_j = \frac{E_{\mathrm{mix},k}^{\mathrm{d}}}{E_{\mathrm{mix}}},\ k = 1, 2, ..., K, \end{cases} \tag{11}$$

$$\lambda_j = E(D_j)/E_{\mathrm{mix}}. \tag{12}$$

Apparently, the accuracy of the PSD results calculated by Eq. (11) relates to the decomposition level k. For instance, 7 components of particle sizes need 7 or more decomposed scales. By defining the characteristic parameters as

$$\begin{cases} P_k^{\mathrm{a}}(D_j) = E_k^{\mathrm{a}}(D_j)/E(D_j), \\ P_k^{\mathrm{d}}(D_j) = E_k^{\mathrm{d}}(D_j)/E(D_j), \end{cases} \tag{13}$$

the PSD model can be simplified as

$$\begin{cases} \sum_{j=1}^{N}\lambda_j P_k^{\mathrm{a}}(D_j)x_j = P_{\mathrm{mix},k}^{\mathrm{a}},\ k = K, \\ \sum_{j=1}^{N}\lambda_j P_k^{\mathrm{d}}(D_j)x_j = P_{\mathrm{mix},k}^{\mathrm{d}},\ k = 1, 2, ..., K, \end{cases} \tag{14}$$

where $P_{\mathrm{mix},k}^{\mathrm{a}}$ and $P_{\mathrm{mix},k}^{\mathrm{d}}$ (k=1, 2, …, K) represent the approximation and detail energy fractions of mixed particles in each scale. Since pre-experiments indicated that particles with the same size had the same

characteristic parameters in all scales, the characteristic parameters of the particle j, $P_k^{\mathrm{a}}(D_j)$ (k=K) and $P_k^{\mathrm{d}}(D_j)$ ($k=1,2,\ldots,K$), and those of the mixture $P_{\mathrm{mix},k}^{\mathrm{a}}$ (k=K) and $P_{\mathrm{mix},k}^{\mathrm{d}}$ ($k=1,2,\ldots,K$) can be calibrated through designed experiments. From Eq. (12), we find that the parameter λ_i can be obtained from the ratio of $E(D_i)$ and E_{mix}, which can be obtained in the calibration process in pre-experiment. Subsequently, once the parameter λ_i is given by experimental data, the mass fraction x_i would be calculated by Eq. (14), which is defined as the PSD model.

3 Experimental apparatus

Fig. 2 shows a schematic diagram of the experimental apparatus used in this study. It consists of two parts: a fluidized bed and the AE measurement system. For cold-model equipment, the fluidized bed is made of transparent Plexiglas with an inside diameter of 0.15 m and a height of 2.0 m. The perforated-plate distributor (with a pore diameter of 2.0 mm and an open area ratio of 2.6%) is installed at the bottom. Air was used as fluidization gas and the velocity varied from 0 to 1.1 m/s. For the pilot-scale setup, the fluidized bed is made of stainless steel with a diameter of 4.5 m and a height of 12 m. The superficial gas velocity is 0.6 m/s, and the distributor is perforate plated with an open area ratio of 3.2%.

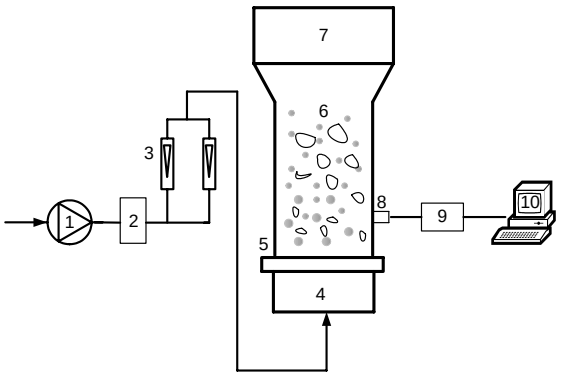

1: Fan; 2: Dryer and heater; 3: Flow meter; 4: Mixing room; 5: Distributor; 6: Fluidized bed; 7: Expanding section; 8: Acoustic sensor; 9: Data acquisition system; 10: Computer

Fig. 2 Schematic diagram of the cold-model of fluidized bed reactor

The acoustic shot noise (the acoustic signals generated from the particle shooting) on-line collection and analysis system developed by the UNILAB Research Center of Chemical Engineering in Zhejiang University, China consists of the data collection system and the computer. The data collection system includes an AE signal sensor, an amplifier, and an analog to digital conversion. The AE sensor is a piezoelectric accelerometer, which is broadly used in collecting the acceleration of vibration without the noise transferred via the air (PXR 15, 50–250 kHz, 150 dB). AE sensors were mounted on the outer wall of the column at 0.1 m above the distributor in the experimental apparatus and 1 m in the industrial fluidized bed, respectively, with a sampling frequency of 500 kHz.

4 Results and discussion

4.1 Applications of PSD model

4.1.1 Influence of decomposed level k

In this study, three kinds of polyethylene particles with different PSDs were chosen for the experiments: linear low density polyethylene (LLDPE, PSD of the large particles dominated), high density polyethylene (HDPE, PSD of two peaks), and bimodal PE (fine particles dominated). The physical properties of experiment particles are shown in Table 1. As the decomposition level changed with k=1, 2, …, 16, the PSDs of LLDPE, HDPE, and bimodal PE were calculated through PSD model. All of the results suggested that the difference between the estimated value and the actual value decreased as the analysis scale increased, and it reached a minimum at a special scale level, which is called the optimum scale. In our case, the optimum scale is found to be 7 by comparing the estimated value from PSD model with the sieving method, with the maximum error being 4.3%. The frequency ranges of 7 scales were shown in Table 2.

Table 1 Physical properties of particles

Material	Particle density (kg/m^3)	Mean particle size (mm)	Young's modulus (N/m^2)
LLDPE	920	0.710	10^9
HDPE	961	0.670	10^9
Bimodal PE	940	0.365	10^9

Table 2 Frequency ranges of 7 scales wavelet transform

Energy distribution	Frequency range (kHz)	Energy distribution	Frequency range (kHz)
d_1	250–500	d_5	15.63–31.25
d_2	125–250	d_6	7.82–15.63
d_3	62.5–125.0	d_7	3.91–7.82
d_4	31.25–62.50	a_7	0–3.91

4.1.2 PSD model for lab and plant setups

Experiments were carried out in cold-model equipment and pilot-scale setup, the superficial velocity of gas U was kept constant at 0.6 m/s, and the weights of the fluidized particles were 500 and 2000 g, respectively. In plant setups, e.g., LLDPE particles, seven kinds of particles were chosen previously for the experiment, whose particle sizes were 0.14 mm (j=1), 0.18 mm (j=2), 0.36 mm (j=3), 0.50 mm (j=4), 0.71 mm (j=5), 1.19 mm (j=6), and 2.00 mm (j=7) by the sieving method. The mixture of seven kinds of particles and the single particle were fluidized, and the AE signals were obtained. The energy distributions of each particle in all scales $P_k^{\mathrm{d}}(D_j)$ (k=1–7) in detail part and $P_k^{\mathrm{a}}(D_j)$ (k=7) in approximation part were calibrated by experimental data (Fig. 3a). Fig. 3b illustrated the energy distribution of the mixture in all scales $P_{\mathrm{mix},k}^{\mathrm{d}}$ (k=1–7) and $P_{\mathrm{mix},k}^{\mathrm{a}}$ (k=7). Since λ_i can be calculated by experimental data, the mass fraction of each particle x_j can be deduced by the PSD model as demonstrated in Fig. 3.

Concerning the influence of particle kinds on the results, AE signals from three different polyethylene powders of LLDPE, HDPE, and bimodal PE were obtained for experiments both in cold-model equipment and industrial fluidized beds **(**Fig. 4). The results from the PSD method were in high agreement with the sieving method for all three particles. The corresponding deviations in cold-model equipment were 3.2%, 5.3%, and 8.8%, while for the industrial setup the average deviations were 6.2%, 8.3%, and 15.8%, respectively.

The above illustration for different particles demonstrated that PSD model based on AE method is suitable for on-line PSD prediction and showed a reliable accuracy.

4.2 Parameter revision of PSD model

By comparing different values of results between the PSD model and the sieving method for three different particles, we could find that the difference of bimodal PE system is obviously greater than those of LLDPE and HDPE both in plant and laboratory (Fig. 4). The reason can be that bimodal PE particles have lower crystallization (the crystallization level is low in the process of production) and less molecular weight, which lead to lower mechanical strengths (such as elasticity and Young's modulus). Moreover, the decrease in Young's modulus of the particles affects the energy ratio of a single particle to mixed particle λ_j. In other words, the decrease affects the contribution of energy of each single PE particle to the total energy of mixed PE particles, which

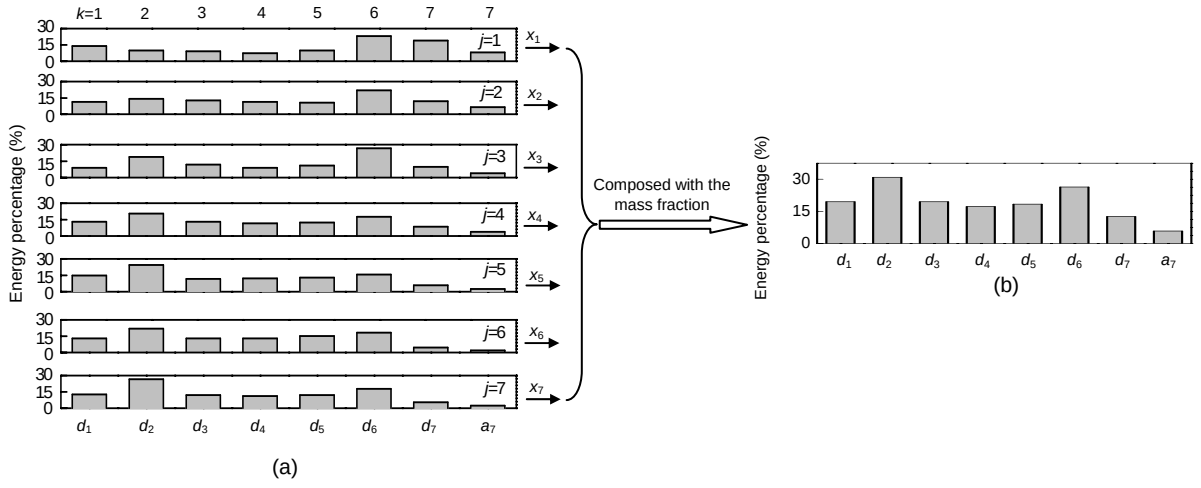

Fig. 3 Energy distribution of single particles (LLDPE) (a) and the mixture (b) in seven scales in experimental apparatus (U=0.6 m/s; ρ_s=920 kg/m^3)

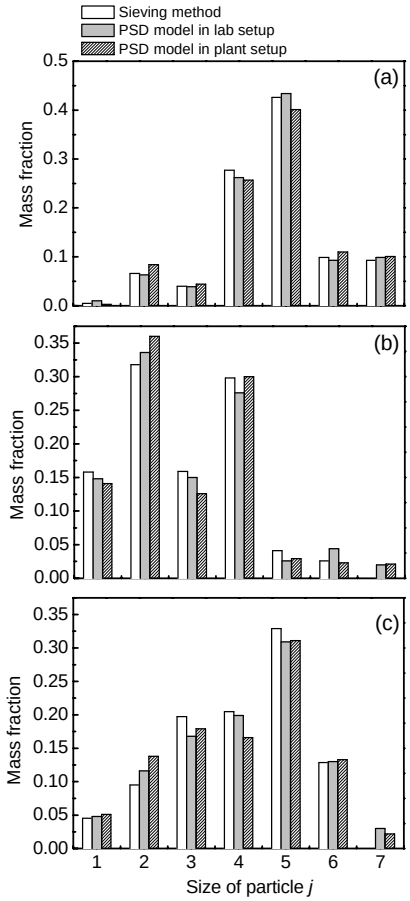

Fig. 4 Comparison of PSD results from the PSD model and sieving method for LLDPE (a), HDPE (b), and bimodal PE (c)
U=0.6 m/s; ρ_s=920 kg/m^3

results in less accuracy for bimodal PE particle system. Conversely, the fluidized particles in the plant setup under the condition of 85–100 °C whose Young's moduli are obviously lower than those in the laboratory will also cause the change of λ_j. This explanation supports the result that the PSD errors in the plant setup are bigger than those in the laboratory. To sum up, λ_j varies and affects the accuracy of the PSD model under special conditions. As a consequence, the parameter λ_j in the PSD model must be revised before practical application to obtain an accurate result.

Fig. 5 shows the energy distribution of acoustic signals of LLDPE particles in laboratory and plant setups when signals are decomposed into 7 scales. It is demonstrated that the energy distributions in both situations are similar. We can also find that the energy percentage of the plant setup is higher than those of the laboratory in low frequency parts (d_5 and d_6). This phenomenon is caused by the increase of temperature in the plant setup, which leads to the change of Young's modulus and parameter λ_j. According to Landau (1970) and Ma (1983), the ratio of elastic modulus at the temperatures of 25 and 85 °C is 0.77 for PE particles. Therefore, the ratio of frequency in the laboratory and plant setups is given as $f_{\text{lab}}/f_{\text{plant}}$=1.11 according to the relationship between the frequency and elastic modulus parameter $f \propto D^{-0.4}$ (Ni *et al.*, 1997). This also indicates that the frequency of acoustic signals in plant is lower than that in laboratory; that is to say, the data calculated from a laboratory setup (energy ratio λ_j and characteristic parameters $P_{k,\text{d}}(D)$ and $P_{k,\text{a}}(D)$) are also suitable for a plant setup through revision.

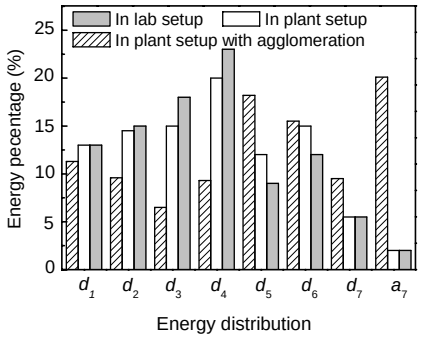

Fig. 5 Comparison of the energy percentage of LLPDE in experimental apparatus, industrial unit, and agglomeration appeared
U=0.6 m/s; ρ_s=920 kg/m^3

4.3 Forecast of the agglomeration in gas-solid fluidized beds

The control of fluidization quality is already known to play an important role in the processes of industry production in a gas-solid fluidized bed. In nearly all these processes, it is of crucial importance to prevent the onset of agglomeration. Under most fluidization conditions, the onset of agglomeration always results in a rapid decrease of frequency of acoustic signals (Jiang *et al.*, 2007), which provides important information about detection of the appearance of agglomeration. As shown in Fig. 5, compared with normal operation, the energy percentages under agglomeration conditions seem to have an increase in low frequency parts (a_7, d_7, d_6, and d_5) whose energies are mostly attributed to the impact of particles with a large size according to the fact that the collision of particles with different sizes leads to

specific frequency ranges. Meanwhile, the energy percentages in high frequency parts (d_1–d_4) decrease correspondingly. That is, the energy distribution with agglomeration in all scales is distinctly different from that under normal operations, which means that different operational conditions result in different PSD. Eventually, the mass fraction of particles with sizes larger than 2.00 mm under abnormal conditions is calculated as 27.8% through the PSD model, which greatly exceeds the value of 9.7% under normal conditions. From another point of view, high percentage of particles with a large size also testifies the existence of agglomeration. Also, the on-line radiation measurement and sampling methods proved the above conclusion, and the fluidized bed was used to detect the existence of agglomeration with a size of 50 mm. In summary, the results indicated that the PSD model based on the AE method can also be applied to the fluidization systems for flow quality detection, and the results can be used to predict the onset of agglomeration by abnormal PSD. This proposed measurement shows sufficient reason and accuracy in the range of experimental conditions analyzed and plays an important role in practical production.

5 Conclusions

In this paper, we have presented a PSD model based on the AE method and multi-scale wavelet decomposition analysis for on-line PSD determination. Experiments were undertaken both in laboratory and plant gas-solid fluidized setups. The results showed that the PSD model revealed the quantitative relationship between the energy distribution of AE signals in different decomposition scales and the PSD, which proved the feasibility of the PSD model. To our delight, the results from the PSD model agreed well with the sieving method for three kinds of experimental particles. Comparing the differences between the results under cold-model and pilot condition, the parameters of the PSD model were calibrated and revised, which ensures the accuracy and practical applications of the PSD model in a pilot-scale process. Moreover, the PSD model also proved to be suitable for detecting the onset of agglomeration. With the presence of agglomeration, energy percentages have an increase in low frequency parts (a_7, d_7, d_6, and d_5) and a decrease in high frequency parts (d_1–d_4) correspondingly, which leads to abnormal PSD. That is, PSD model based on AE technique and energy analysis can be successfully used to monitor the fluidization quality and detect the unstable condition in gas-solid fluidized systems by abnormal PSD, which plays an important role in practical production.

Acknowledgements

It is a pleasure to acknowledge Ms. Xiao-jing JIANG and Dr. Xian-bo YU, Department of Chemical and Biological Engineering of Zhejiang University, China. The field data presented here cannot have been accomplished without their assistance.

References

Allen, T., 1990. Particle Size Measurement (4th Ed.). Chapman & Hall, London, UK, p.59-63.

Boyd, J.W.R., Varley, J., 2001. The uses of passive measurement of acoustic emissions from chemical engineering processes. *Chemical Engineering Science*, **56**(5):1749-1767. [doi:10.1016/S0009-2509(00)00540-6]

Braatz, R.D., 2002. Advanced control of crystallization processes. *Annual Reviews in Control*, **26**(1):87-99. [doi:10.1016/S1367-5788(02)80016-5]

Cody, G.D., Goldfarb, D.J., Storch, G.V., Norris, A.N., 1996. Particle granular temperature in gas fluidized beds. *Powder Technology*, **87**(3):211-232. [doi:10.1016/0032-5910(96)03087-2]

Cody, G.D., Bellows, R.J., Goldfarb, D.J., Wolf, H.A., Storch, G.V., 2000. A novel non-intrusive probe of particle motion and gas generation in the feed injection zone of the feed riser of a fluidized bed catalytic cracking unit. *Powder Technology*, **110**(1-2):128-142. [doi:10.1016/S0032-5910(99)00275-2]

Franklin, J.A., Katsabanis, T., 1996. Measurement of Blast Fragmentation. Balkema Press, Rotterdam, the Netherlands, p.79-82.

Fuerstenau, M.F., Kenneth, N.H., 2003. Principle of Mineral Processing. SME Press, Colorado, USA, p.9-60.

Haar, D.T., 1954. Elements of Statistical Mechanics. Rhinehart Press, New York, USA, p.468-469.

Halstensen, M., Esbensen, M., 2000. New developments in acoustic chemometric prediction of particle size distribution—'the problem is the solution'. *Journal of Chemometrics*, **14**(5-6):463-481. [doi:10.1002/1099-128X(200009/12)14:5/6<463::AID-CEM628>3.0.CO;2-Y]

He, Y.J., Wang, J.D., Cao, Y.J., Yang, Y.R., 2009. Resolution of structure characteristics of AE signals in multiphase flow system-from data to information. *AIChE Journal*, **55**(10):2563-2577. [doi:10.1002/aic.11878]

Hunter, G.C., McDermott, C., Miles, N.J., Singh, A., Scoble,

M.J., 1990. A review of image analysis techniques for measuring blast fragmentation. *Mining Science and Technology*, **11**(1):19-36. [doi:10.1016/0167-9031(90)80003-Y]

Jiang, X.J., Wang, J.D., Jiang, B.B., Yang, Y.R., Hou, L.X., 2007. Study of power spectrum of acoustic emission (AE) by accelerometers in fluidized beds. *Industrial and Engineering Chemistry Research*, **46**(21):6904-6909. [doi:10.1021/ie070457i]

Landau, L.D., 1970. Theory of Elasticity. Pergamon, Oxford, UK, p.97-102.

Lange, T.B., 1988. Real-Time Measurement of the Size Distribution of Rocks on a Conveyor Belt. Proceedings IFAC Applied Measurements in Mineral and Metallurgical Processing, Transvaal, South Africa, p.25-36.

Larsen, P.A., Rawlings, J.B., Ferrier, N.J., 2006. An algorithm for analyzing noisy, in situ images of high-aspect-ratio crystals to monitor particle size distribution. *Chemical Engineering Science*, **61**(16):5236-5248. [doi:10.1016/j.ces.2006.03.035]

Lin, C.L., Yen, Y.K., Miller, J.D., 1995. On-Line Particle Size Measurement—Industrial Testing. SME Annual Meeting, Denver, Colorado, USA, p.95-241.

Lin, C.L., Yen, Y.K., Miller, J.D., 2000. Plant-site evaluations of the OPSA system for on-line particle size measurement from moving belt conveyors. *Minerals Engineering*, **13**(8-9):897-909. [doi:10.1016/S0892-6875(00)00077-7]

Ma, D.Y., 1983. Acoustics Handbook. Science Press, Beijing, China, p.58-60 (in Chinese).

Monoro, J.J., Gonzalez, E., 1993. New Analytical Techniques to Evaluate Fragmentation Based on Image Analysis by Computer Methods. Proceedings of the 4th International Symposium on Rock Fragmentation by Blasting, Vienna, Austria, p.309-316.

Mylvaganam, S., 2003. Some applications of acoustic emission in particle science and technology. *Particulate Science and Technology*, **21**(3):293-301. [doi:10.1080/02726350307485]

Naito, M., Hayakawa, O., Nakahira, K., Mori, H., Tsubaki, J., 1998. Effect of particle shape on the particle size distribution measured with commercial equipment. *Powder Technology*, **100**(1):52-60. [doi:10.1016/S0032-5910(98)00052-7]

Ni, J.R., Han, P., Zhang, R., 1997. Variations of sediment characteristics in the middle reach of Yellow river with respect to regional water and soil conservations I: sediment size distributions. *Journal of Natural Resources*, **12**(1):1-9.

Peng, Y.H., 2000. Wavelet Transform and the Application in Engineering. Science Press, Beijing, China, p.153-160 (in Chinese).

Ren, C.J., Jiang, X.J., Wang, J.D., Yang, Y.R., Zhang, X.H., 2008. Determination of critical speed for complete solid suspension using acoustic emission method based on multiscale analysis in stirred tank. *Industrial and Engineering Chemistry Research*, **47**(15):5323-5327. [doi:10.1021/ie0714347]

Wang, J.D., Yang, Y.R., Ge, P.F., Shu, W.J., Hou, L.X., 2007. Measurement of the fluidized velocity in gas-solid fluidized beds based on AE signal analysis by wavelet packet transform. *Science in China Series B: Chemistry*, **50**(2):284-289. [doi:10.1007/s11426-007-0037-5]

Wang, J.D., Ren, C.J., Yang, Y.R., 2010. Characterization of flow regime transition and particle motion using acoustic emission measurement in a gas-solid fluidized bed. *AIChE Journal*, **56**(5):1173-1183. [doi:10.1002/aic.12071]

Worlitschek, J., Hocker, T., Mazzotti, M., 2005. Restoration of PSD from chord length distribution data using the method of projections onto convex sets. *Particle and Particle Systems Characterization*, **22**(2):81-98. [doi:10.1002/ppsc.200400872]

Wu, Z.H., 1999. College Physics. Zhejiang University Press, Hangzhou, China, p.200-203 (in Chinese).

Xu, R.L., Guida, O.A.D., 2003. Comparison of sizing small particles using different technologies. *Powder Technology*, **132**(2-3):145-153. [doi:10.1016/S0032-5910(03)00048-2]